Electronic Supplementary Material (ESI) for Journal of Materials Chemistry A.

Electronic Supplementary Information

Iodide-Mediated Templating Synthesis of Highly Porous Rhodium Nanospheres for Enhanced Dehydrogenation of Ammonia Borane

Houbing Zou, Bo Jin, Runwei Wang, Yanbo Wu, Hengquan Yang* and Shilun Qiu*

Dr. H. B. Zou, B. Jin, Prof. Y. B. Wu, Prof. H. Q. Yang
School of Chemistry and Chemical Engineering
Shanxi University
92 Wucheng Road, Taiyuan, 030006 (P. R. China)
E-mail: hqyang@sxu.edu.cn

Dr. H. B. Zou, Prof. R. W. Wang, Prof. S. L. Qiu
State Key Laboratory of Inorganic Synthesis and Preparative Chemistry
College of Chemistry
Jilin University
2699 Qianjin Street, Changchun, 130012 (P. R. China)
E-mail: rwwang@jlu.edu.cn
Telephone: +86-431-85168115
Fax numbers: +86-431-85168115

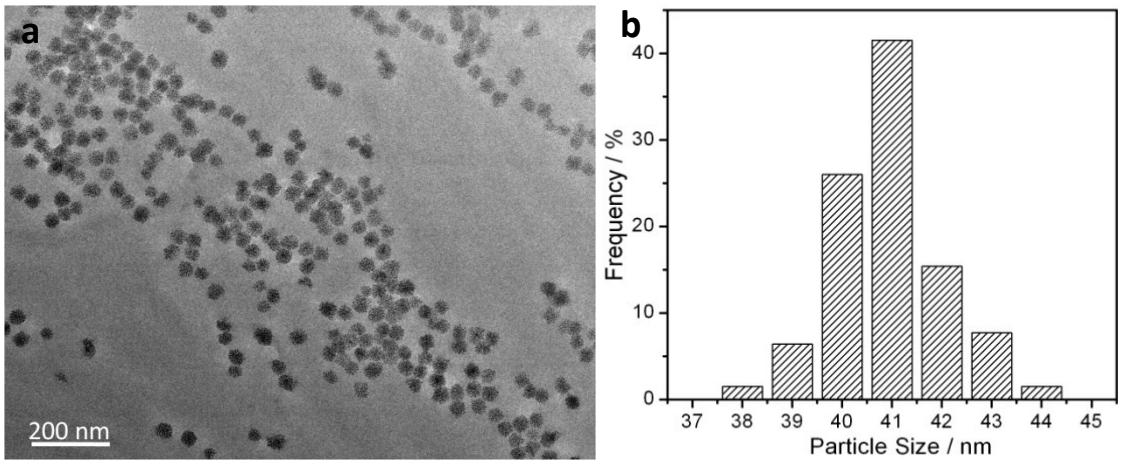

Figure S1. (a) Low-magnification TEM image and (b) size distribution histogram of the highly porous Rh nanospheres (HPRhS).

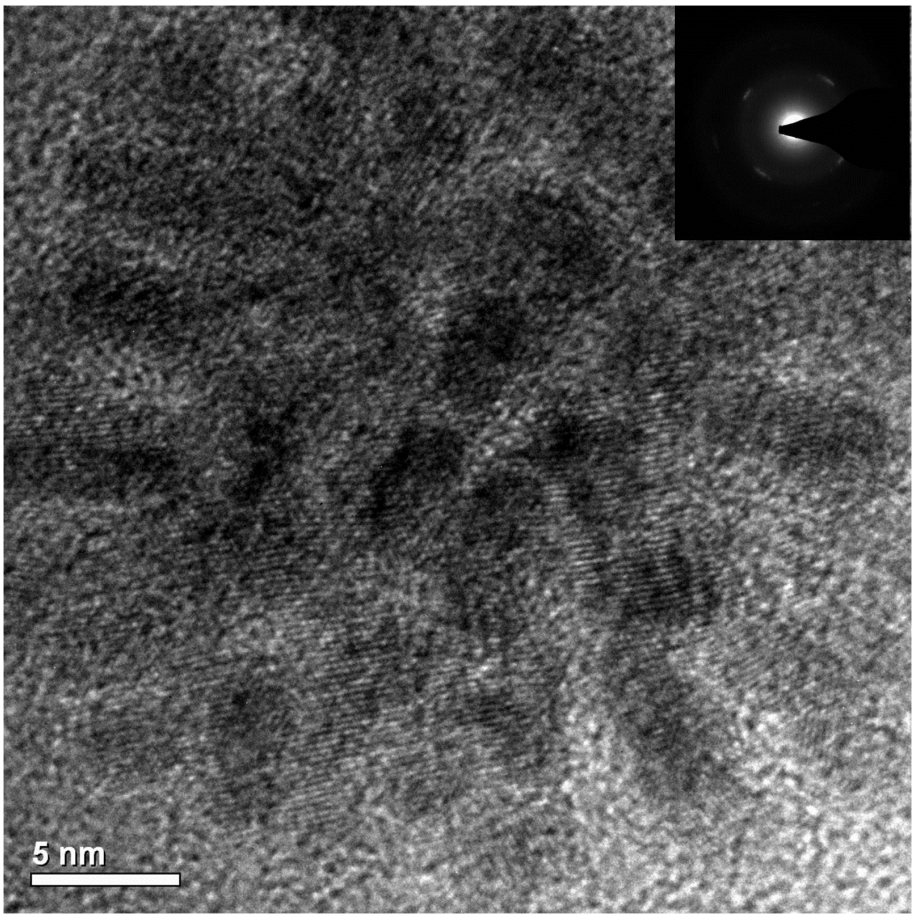

Figure S2. HRTEM image and SAED pattern (the inset) of an individual HPRhS nanoparticle.

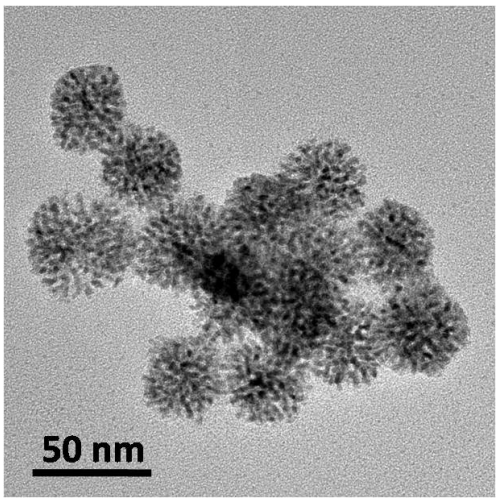

Figure S3. Typical TEM image of the HPRhS sample after sonicating for 3 hours.

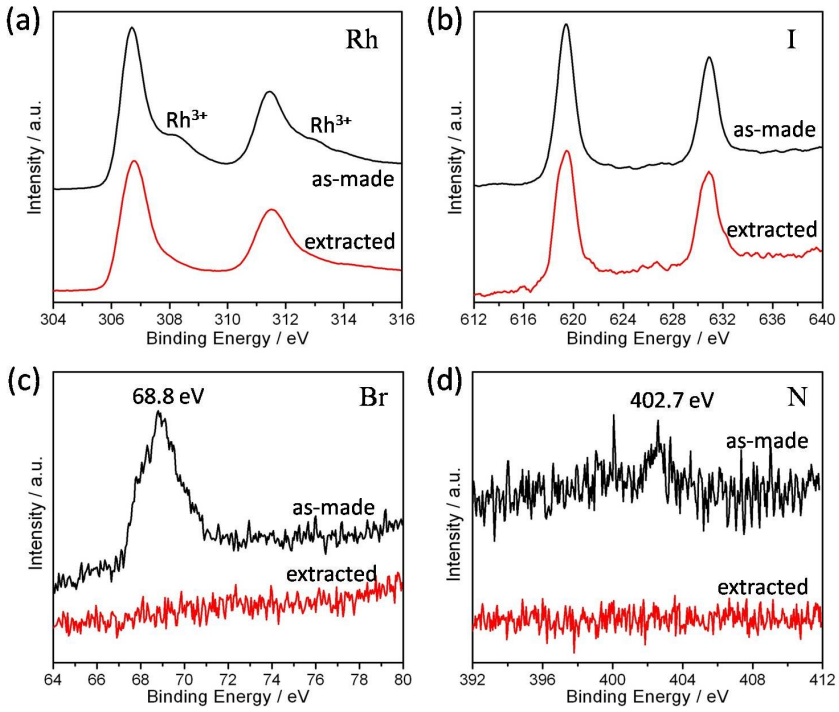

Figure S4. Rh 3d (a), I 3d (b), Br 3d (c) and N 1s (d) XPS sperctra of the as-made HPRhS (black line) and extracted HPRhS (red line).

It can be seen clearly that there is another broad peak at the binding energy of 308.4 eV in the Rh XPS spectrum of as-made sample besides the zerovalent state (306.8 eV), which can be assigned to the Rh^{3+} state. Moreover, I, Br and N elements are also detected in the as-made sample according to their XPS spectra. These results indicate that the surfactant CTAB molecules occupy in the nanopores of as-made HPRhS and there is some unreduced Rh^{3+} absorbing on the nanopore surface. After refluxing as-made material in acid ethanol solution for 12 h twice, only I^- and Rh^0 state can be detected in the extracted sample, which suggest that the surfactant molecules have been removed well and the iodide ion is anchored on the nanopore surface due to its strong chelating capacity, then leading to an open nanopore and a functional pore surface.

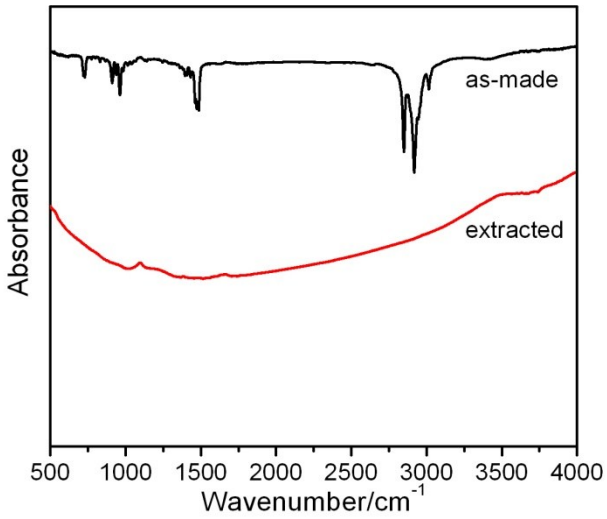

Figure S5. FT-IR sperctra of the as-made HPRhS and extracted HPRhS.

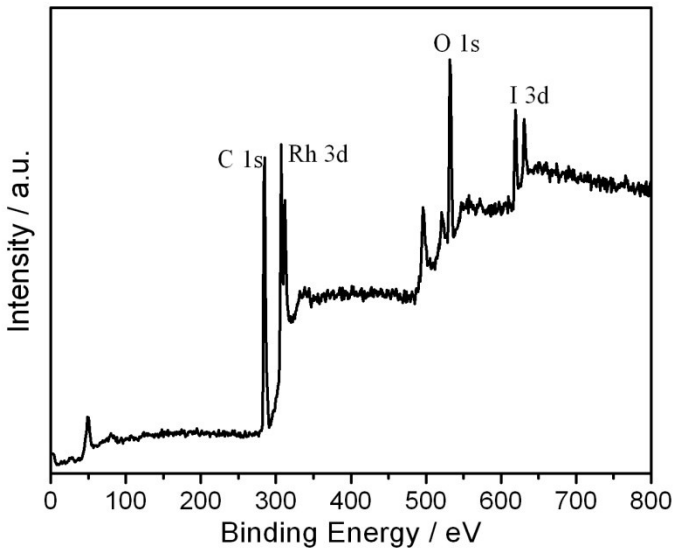

Figure S6. Survey XPS spectrum of the extracted HPRhS.

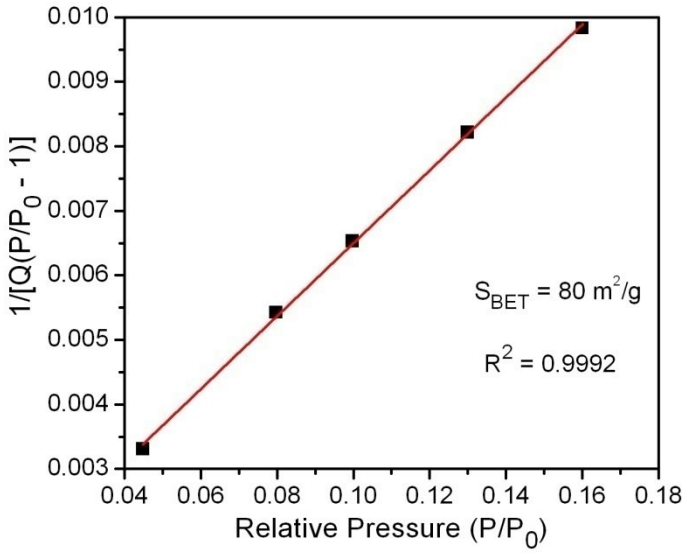

Figure S7. BET plot of the extracted HPRhS sample calculated from the N_2 adsorption isotherm.

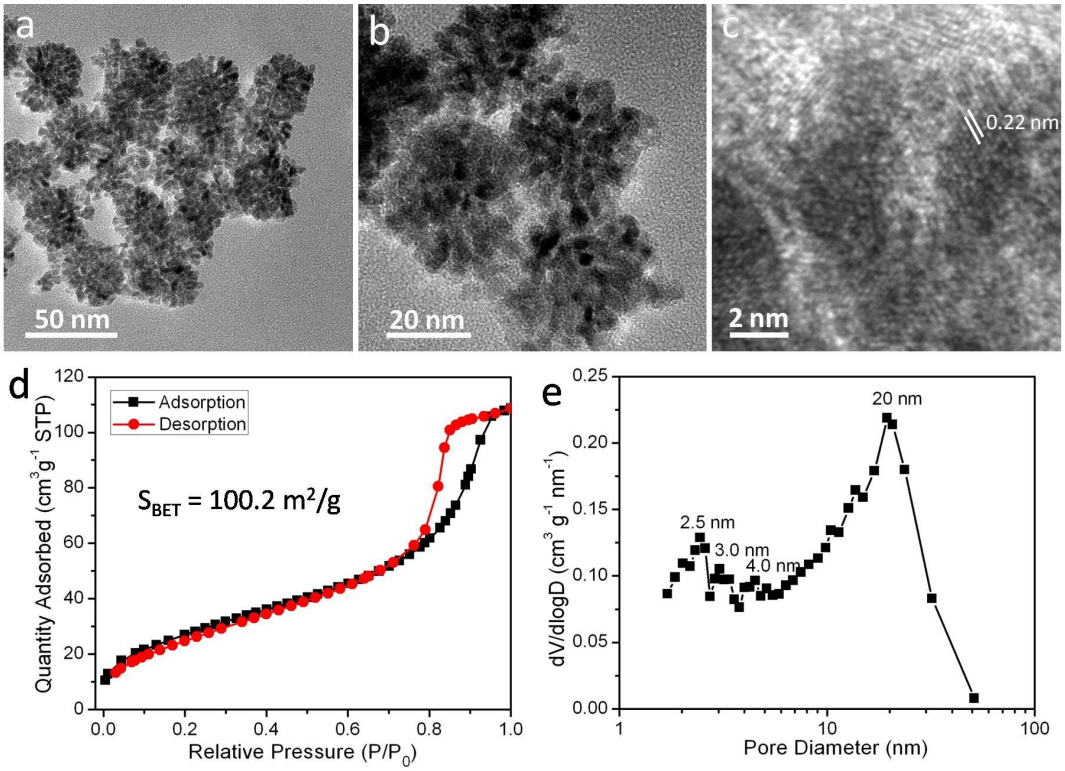

Figure S8. TEM images (a, b, c), N_2 adsorption-desorption isotherms (d) and pore size distribution plot (e) of HPRhS calcinated for 3 hours under air (250 °C). The HRTEM image suggests that the treated HPRhS is still in metal state. The ICP-AES analysis reveals that the molar ratio of Rh to I is 60:1, indicating most of iodide ions have been removed via calcination.

Table S1 BET special surface areas and pore sizes of different nanoporous noble metal nanoparticles

Sample	Pore Size	Method	BET Special Surface Area	References
Mesoporous Pt single crystalline	2.7 nm	Nanocasting from KIT-6	39 $m^2 g^{-1}$	JACS, **2011**, 133, 14526.
Dendritic Pt NPs	2-4 nm	wet chemistry F127 as template	56 $m^2 g^{-1}$	JACS, **2009**, *131,* 9152.
MesoporousPd@PtNPs with concave surface	-	wet chemistry F127 as template	40 $m^2 g^{-1}$	Angew.,**2013**, 52, 13611.
Mesoporous Pt Nanospheres with large mesopores	8-35 nm	wet chemistry PS-b-P2VP-b-PEO as template	30 $m^2 g^{-1}$	Angew.,**2015**, 54, 11073.
Porous Pd nanosphere with perpendicular pore	2-3 nm	wet chemistry HDPC as template	61.2 $m^2 g^{-1}$	Angew.,**2013**, 52, 2520 .
Mesoporous Rh NPs with large mesopores	20 nm	wet chemistry PEO-*b*-PMMAas template	50 $m^2 g^{-1}$	Nature Comm.,**2017**, 8, 15581.
HPRhS-extracted	2-3 nm	wet chemistry $I^-$and CTAB as template	80 $m^2 g^{-1}$	***This work***
HPRhS-calcined	2-4 nm	wet chemistry $I^-$and CTAB as template	100.2 $m^2 g^{-1}$	***This work***

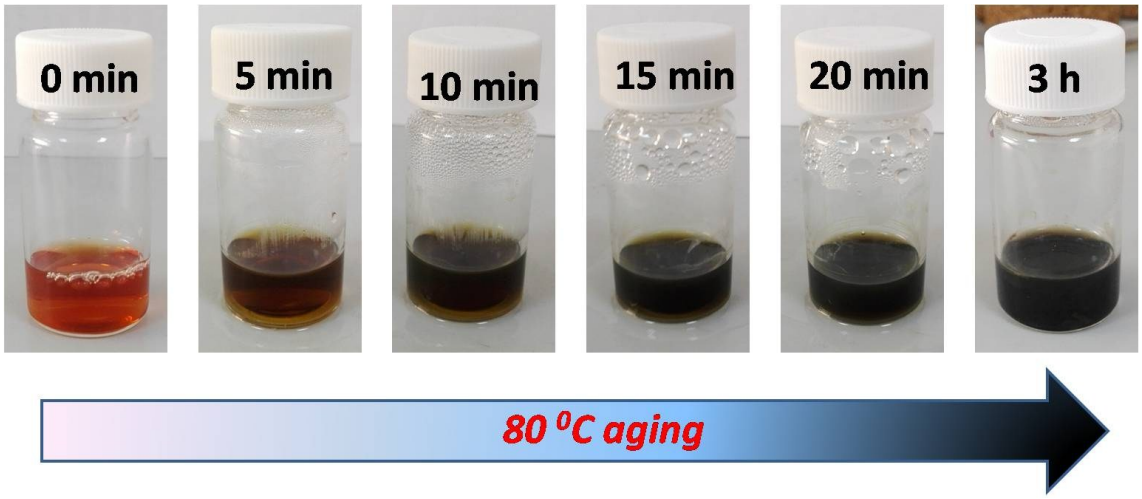

Figure S9. Photographs of the HPRhS sample aging at different reaction times.

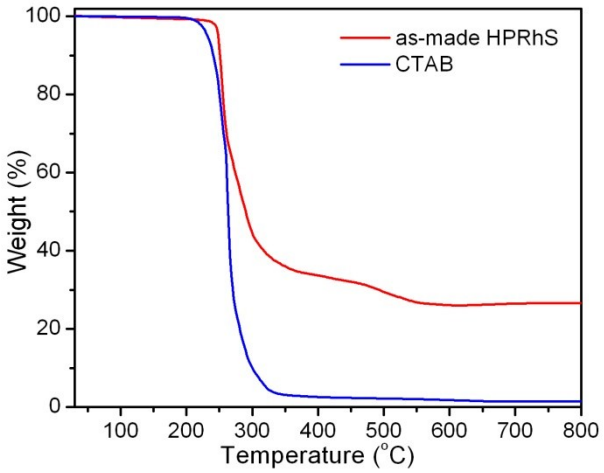

Figure S10. TG curves of the as-made HPRhS and the surfactant CTAB.

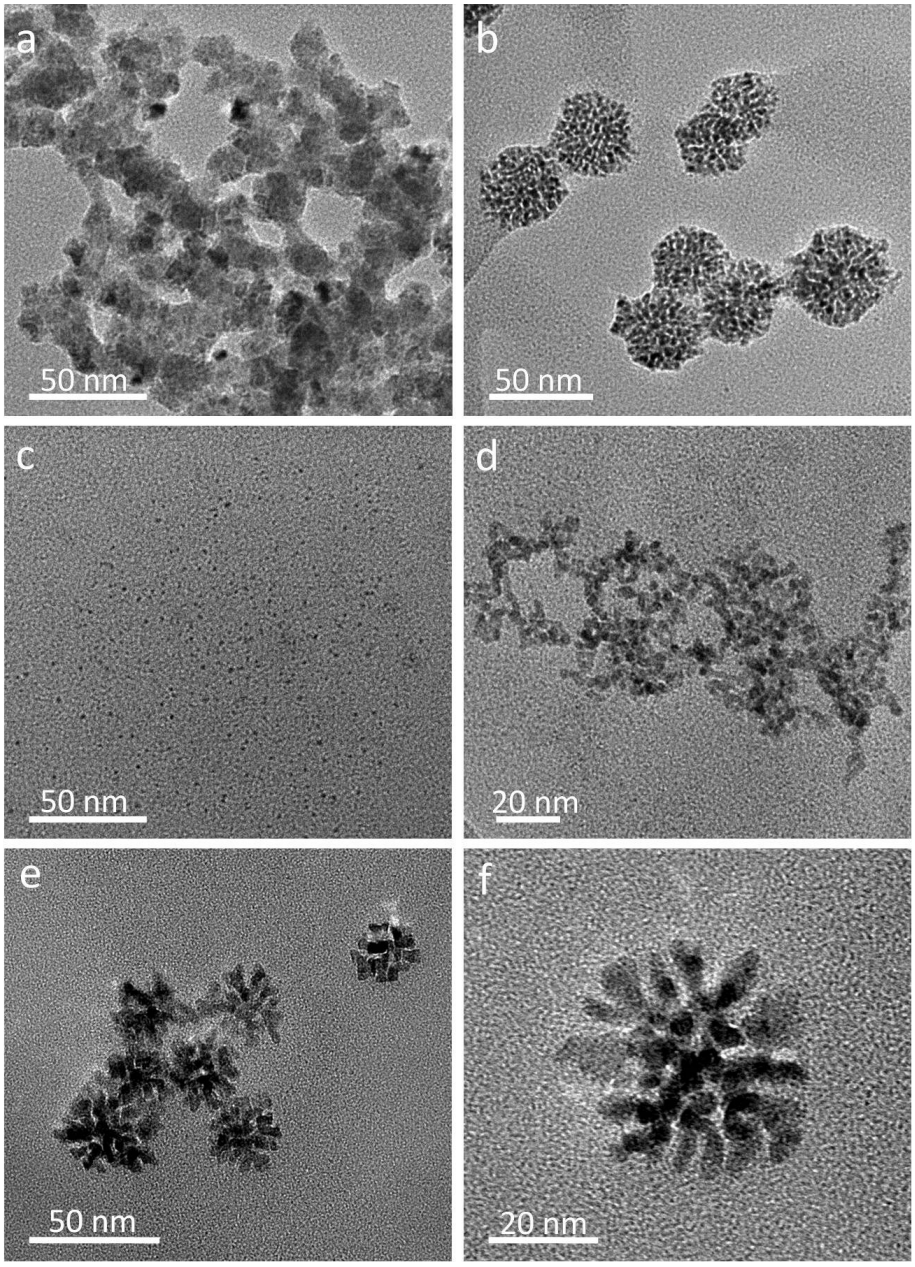

Figure S11. TEM images of the Rh sample prepared at the similar reaction conditions for the typical HPRhS but (a) in the absence of CTAB, (b) using 50 mg of CTAB, (c) using PVP to replace the CTAB, (d) using strong reductant $NaBH_4$ to replace AA and (e, f) using another weak reducing agent HQ to replace AA.

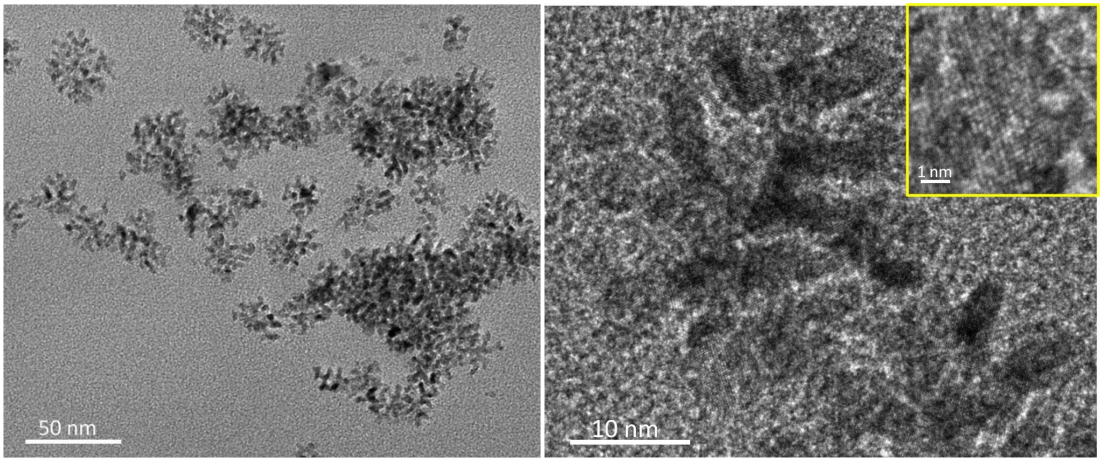

Figure S12. TEM images of the porous Rh nanoparticles prepared under the identical reaction conditions for the typical HPRhS but in the absence of I^-.

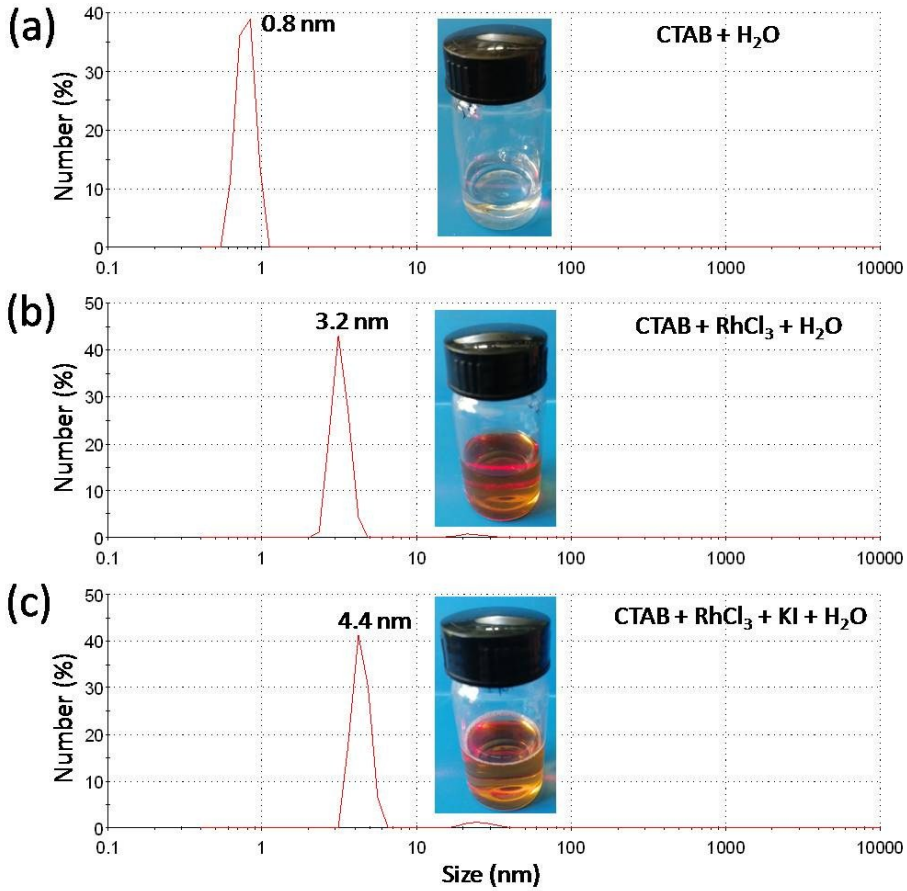

Figure S13. Hydrodynamic diameter determination of CTAB solution, the mixture of precursor and CTAB, and the mixture of precursor, CTAB and KI obtained through dynamic light scattering (DLS). The insets show corresponding Tyndall effect.

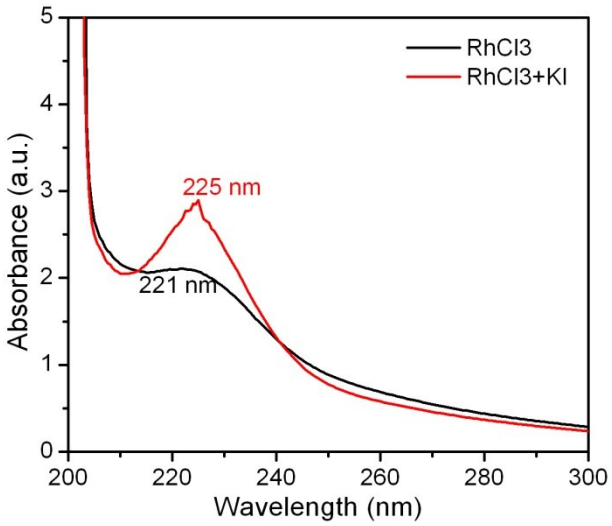

Figure S14. UV-Vis spectra of the $RhCl_3$ aqueous solution and the $RhCl_3$+KI aqueous solution.

After the addition of the iodide ons, the absorbance peak shifted from 221 nm to 225 nm, suggestting that the iodide ions have complexed with the Rh^{3+}. This result reveals that the iodide ions have a stronger chelating capacity due to their stronger electron donating capacity.

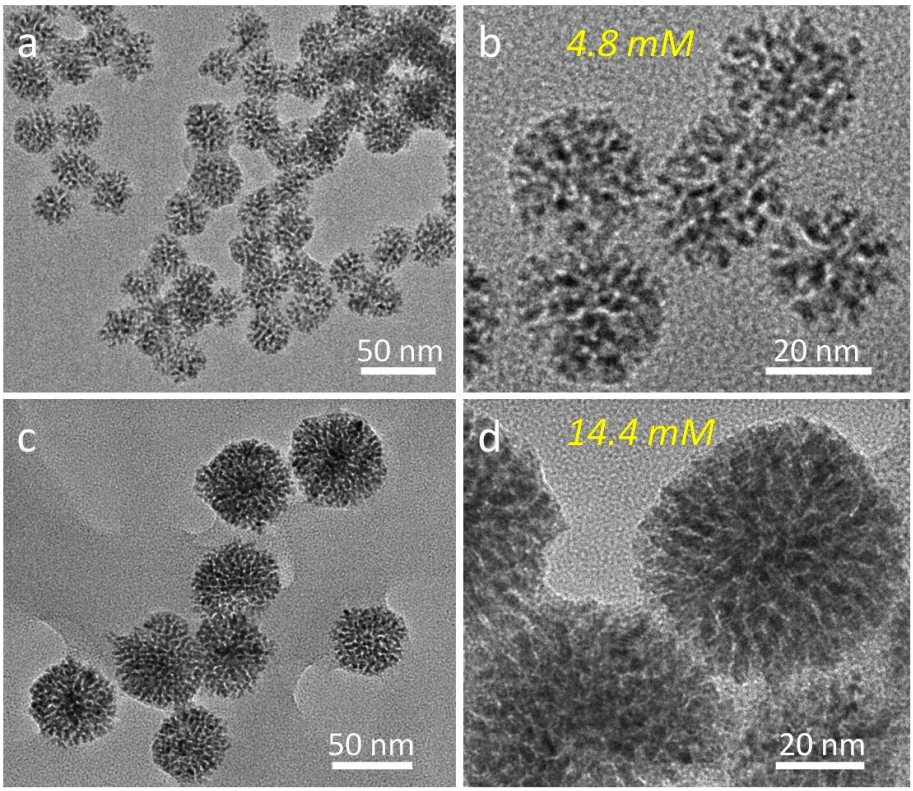

Figure S15. TEM images of HPRhS with tunable particle sizes prepared under different concentrations of $RhCl_3$ precursor: (a, b) 4.8 mM, (c, d) 14.4 mM.

Table S2 Methanolytic dehydrogenation of AB over reported catalysts and our HPRhS.

Catalyst	Temp (°C)	Catalyst/AB molar ratio (mol mol^{-1})	TOF ($mol_{H2} \cdot mol_{cat}^{-1} \cdot min^{-1}$)	References
Rh/nanoSiO_2	25	0.00245	168	Appl. Catal., B **2016**, 181, 716.
Rh/nanoHAP	25	0.00203	147	Int. J. Hydrogen Energy **2015**, 40, 10491.
Rh/Zeolite	25	0.0034	30	Appl. Catal., B **2010**, 93, 387.
Ru/MMT	25	0.003	118.1	Int. J. Hydrogen Energy **2010**, 35, 10317.
Ru/graphene	25	0.003	99.4	Int. J. Hydrogen Energy **2015**, 40, 10856.
PVP-stabilized Ru	25	0.0075	47.7	Catal Today **2011**;170, 93-8.
PVP-stabilized Pd	25	0.005	22.3	Phys. Chem. Chem. Phys. **2009**, 11, 10519.
CuPd/C	25	0.072	53.2	Nanotechnology **2015**, 26, 025401.
CoPd/C	25	0.027	27.7	ACS Catal. **2012**, 2, 1290.
Rh/CC3-R-homo	25	0.0199	215.3 (0.7 min)	JACS, **2015**, 137, 7063.
Rh/CC3-R-hetero	25	0.0199	65.5 (2.3 min)	JACS,**2015**, 137, 7063.
Rh/P(triaz)	25	0.01	260 (1.16 min)	JACS,**2017**, 139, 8971.
Ru NPs@PCC-2	25	0.0035	304.4 (4.5 min)	Chem. **2018**, 4, 555.
HPRhS	25	0.00486	**291.6 (2.11 min)**	***This work***
HPRhS	**0**	0.0097	**50.6 (6.1 min)**	***This work***

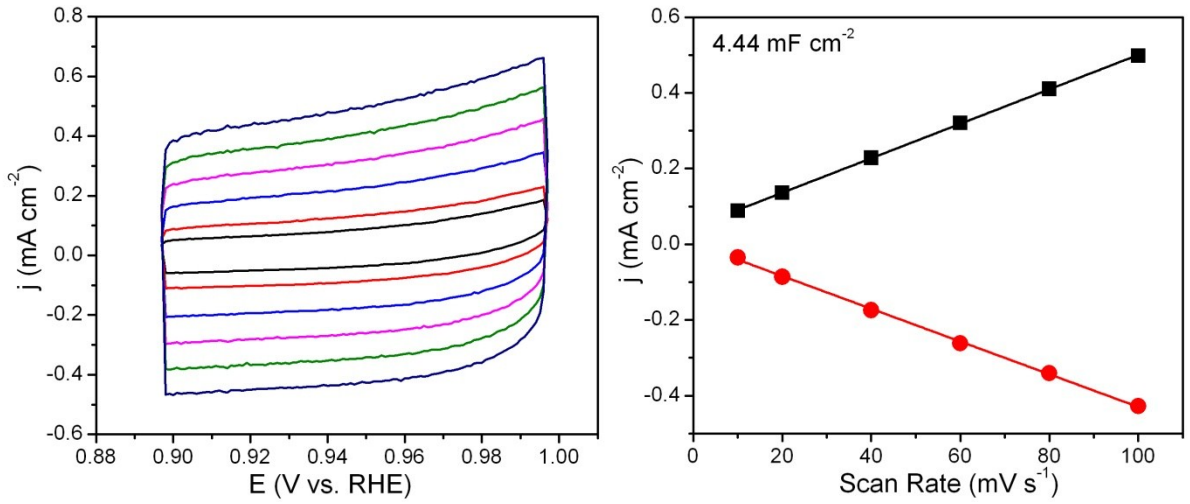

Figure S16. Cyclic voltammogram of our catalyst HPRhS recorded at room temperature in a N_2-purged 0.5 M H_2SO_4 solution.

Our catalyst HPRhS displays an outstandingly high electrochemically active surface area (EASA) of 110 m^2/g, which is much higher than that of most of reported noble metal nanoparticles.[1-3] Such a high EASA indicates that there are high-density of available active sites on the (nanopore) surface.

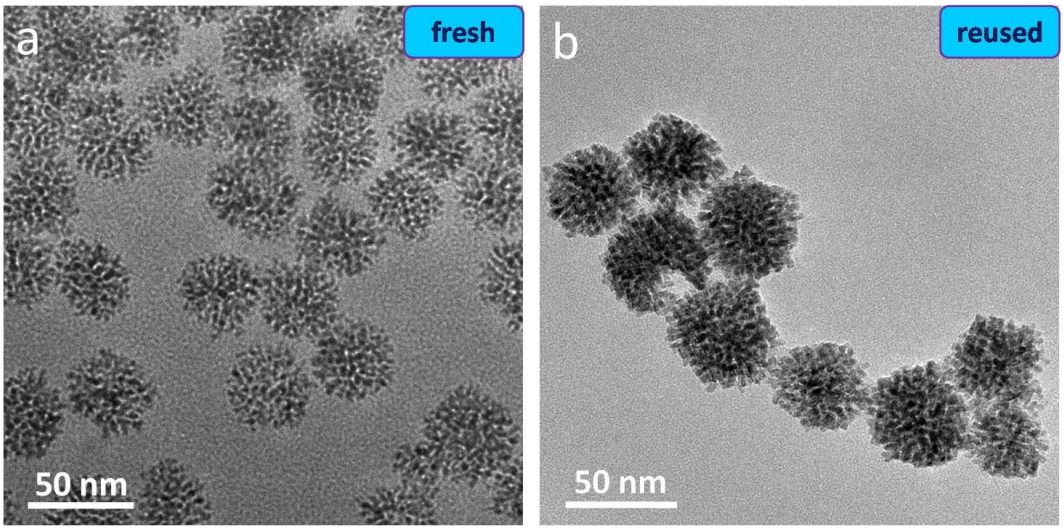

Figure S17. TEM images of the fresh prepared HPRhS (a) and the reused HPRhS (b).

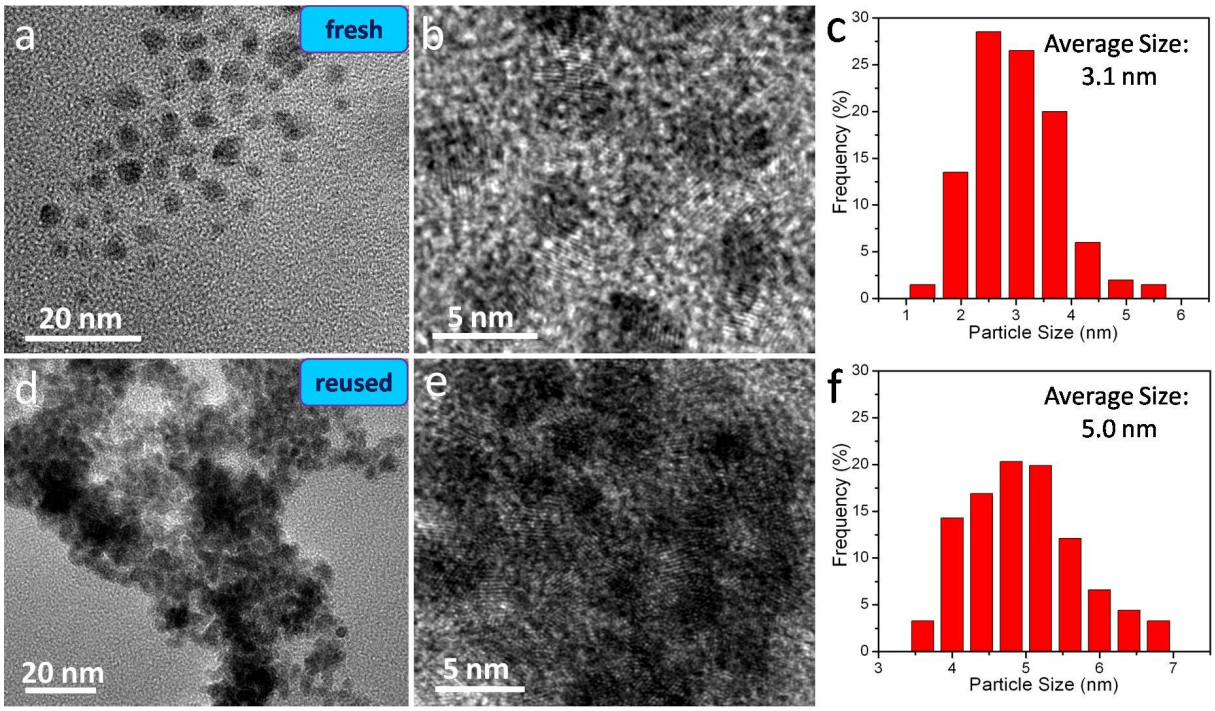

Figure S18. TEM images (a, b, d, e) and particle size distributions (c, f) of the fresh Rh nanoparticles (a, b, c) and the recovered Rh nanoparticles (d, e, f).

References

[1] X. Q. Huang, E. B. Zhu, Y. Chen, Y. J. Li, C.-Y. Chiu, Y. X. Xu, Z. Y. Lin, X. F. Duan, Y. Huang, *Adv. Mater.* **2013**, 25, 2974.

[2] Y. Li, B. P. Bastakoti, V. Malgras, C. Li, J. Tang, J. H. Kim, Y.Yamauchi, *Angew. Chem. Int. Ed.* **2015**, 54, 11073.

[3] X. Huang, Z. Zhao, L. Cao, Y. Chen, E. Zhu, Z. Lin, M. Li, A. Yan, A. Zettl, Y. M. Wang, X. Duan, T. Mueller, Y. Huang, *Science* **2015**, 348, 1230.